Biochemical Pharmacology 158 (2018) 192–200

Contents lists available at ScienceDirect

Biochemical Pharmacology

journal homepage: www.elsevier.com/locate/biochempharm

Evaluating the abilities of diverse nitroaromatic prodrug metabolites to exit a model Gram negative vector for bacterial-directed enzyme-prodrug therapy

Jasmine V.E. Chan-Hyams[a,b], Janine N. Copp[a,b,c], Jeff B. Smaill[d,e], Adam V. Patterson[d,e], David F. Ackerley[a,b,e,*]

[a] School of Biological Sciences, Victoria University of Wellington, Wellington 6012, New Zealand
[b] Centre for Biodiscovery, Victoria University of Wellington, Wellington 6012, New Zealand
[c] Michael Smith Laboratories, University of British Columbia, Vancouver, BC, V6T 1Z4, Canada
[d] Auckland Cancer Society Research Centre, School of Medical Sciences, University of Auckland, Auckland 1023, New Zealand
[e] Maurice Wilkins Centre for Molecular Biodiscovery, School of Biological Sciences, University of Auckland, Auckland 1010, New Zealand

ARTICLE INFO

Keywords:
BDEPT
GDEPT
Cancer gene therapy
Nitroreductase
Bystander effect

ABSTRACT

Gene-directed enzyme-prodrug therapy (GDEPT) employs tumour-tropic vectors including viruses and bacteria to deliver a genetically-encoded prodrug-converting enzyme to the tumour environment, thereby sensitising the tumour to the prodrug. Nitroreductases, able to activate a range of promising nitroaromatic prodrugs to genotoxic metabolites, are of great interest for GDEPT. The bystander effect (cell-to-cell transfer of activated prodrug metabolites) has been quantified for some nitroaromatic prodrugs in mixed multilayer human cell cultures, however while these provide a good model for viral DEPT (VDEPT) they do not inform on the ability of these prodrug metabolites to exit bacterial vectors (relevant to bacterial-DEPT (BDEPT)). To investigate this we grew two *Escherichia coli* strains in co-culture; an activator strain expressing the nitroreductase *E. coli* NfsA and a recipient strain containing an SOS-GFP DNA damage responsive gene construct. In this system, induction of GFP by reduced prodrug metabolites can only occur following their transfer from the activator to the recipient cells. We used this to investigate five clinically relevant prodrugs: metronidazole, CB1954, nitro-CBI-DEI, and two dinitrobenzamide mustard prodrug analogues, PR-104A and SN27686. Consistent with the bystander efficiencies previously measured in human cell multilayers, reduced metronidazole exhibited little bacterial cell-to-cell transfer, whereas nitro-CBI-DEI was passed very efficiently from activator to recipient cells post-reduction. However, in contrast with observations in human cell multilayers, the nitrogen mustard prodrug metabolites were not effectively passed between the two bacterial strains, whereas reduced CB1954 was transferred efficiently. Using nitroreductase enzymes that exhibit different biases for the 2- *versus* 4-nitro substituents of CB1954, we further showed that the 2-nitro reduction products exhibit substantially higher levels of bacterial cell-to-cell transfer than the 4-nitro reduction products, consistent with their relative bystander efficiencies in human cell culture. Overall, our data suggest that prodrugs may differ in their suitability for VDEPT *versus* BDEPT applications and emphasise the importance of evaluating an enzyme-prodrug partnership in an appropriate context for the intended vector.

1. Introduction

Gene-directed enzyme-prodrug therapy (GDEPT) is a targeted cancer therapy that typically uses engineered viral (i.e., VDEPT) or bacterial (BDEPT) vectors to deliver a therapeutic enzyme directly to tumour cells. This enzyme activates a prodrug to one or more cytotoxic metabolites [8]. For example, reduction of a nitroaromatic prodrug by a nitroreductase causes a shift in electron density that typically converts the prodrug into an electrophilic genotoxin, which then generates DNA adducts or cross-links that result in tumour cell death [29].

Bacteria offer several advantages as vectors for cancer gene therapy. For example, bacteria are easily manipulated to generate exogenous products of therapeutic relevance, to improve their tumour selectivity, or to express prodrug activating enzymes and reporter proteins for

* Corresponding author at: School of Biological Sciences, Victoria University of Wellington, Wellington 6012, New Zealand.
E-mail address: david.ackerley@vuw.ac.nz (D.F. Ackerley).

https://doi.org/10.1016/j.bcp.2018.10.020
Received 5 September 2018; Accepted 17 October 2018
Available online 21 October 2018
0006-2952/

visual confirmation of treatment location and therapeutic outcome [11,17,9]. Different types of bacteria have different mechanisms of achieving tumour specificity. Obligate anaerobes such as Gram-positive *Clostridium* species can form spores that are only able to germinate inside the anoxic regions of tumours [20]. In contrast, facultative anaerobes, such as Gram-negative *Salmonella* and *Escherichia,* accumulate inside tumours for several reasons: protection from the immune system, positive chemotaxis towards resources inside the tumour micro-environment and entrapment in the chaotic vasculature of tumours [11,17,9]. Bacteria offer one additional key advantage over their viral vector counterparts – bacterial infection during cancer therapy can readily be controlled by antibiotics [11,20,17].

Critical to the success of GDEPT strategies is the bystander effect, which occurs when an activated chemotherapeutic diffuses from the activating cell to neighbouring tumour cells [6]. This phenomenon was described by Freeman et al. [12], who observed that having only 10% of a mixed tumour xenograft cell population expressing the herpes simplex virus thymidine kinase gene was sufficient to lethally sensitise the entire tumour to the prodrug ganciclovir. The bystander effect of the activated metabolites of ganciclovir is mediated via gap junctions [12,19]), however more lipophilic cytotoxins including many nitroreductase-activated drugs can also manifest a bystander effect via passive diffusion [7,6]. In VDEPT, which relies on expression of a prodrug activating enzyme by the cancer cell itself (Fig. 1A), a strong bystander effect can overcome the inefficiency of viral gene transduction, which is unlikely to exceed 10% of target tissue in the clinic [6]. The bystander effect is even more critical when using bacterial vectors for GDEPT, as the success of the therapy depends entirely upon transport of the activated cytotoxin out of the activating bacterial cell and into the surrounding cancer tissue (Fig. 1B), and failure to exit the vector may result in sterilisation of the bacteria within the tumour.

To quantify the levels of cell-to-cell transfer of the reduced metabolites of nitroaromatic prodrugs between human tumour cells, Wilson et al. [30] developed a mixed multilayer cell culture system, comprising a small proportion of “activator” cells that had been transfected with a nitroreductase together with a large majority of untransfected “recipient” cells. This system has been used to evaluate the relative bystander effect efficiency of diverse nitroaromatic prodrug metabolites. However, we considered that a strong bystander effect measured in human cell culture might not accurately predict the ability of these prodrugs to exit bacterial activator cells, owing to the different transporter systems and cell wall structures. To investigate this, we adapted a previously developed *E. coli* DNA damage responsive GFP reporter strain [4] (Fig. 1C), to detect nitroaromatic prodrug metabolites generated by a co-cultured strain expressing a strong nitroreductase.

2. Materials and methods

2.1. Chemicals and growth media

Unless otherwise stated, chemicals used in this study were obtained from Sigma–Aldrich (St. Louis, MO), including the prodrug metronidazole (2-(2-methyl-5-nitro-1*H*-imidazol-1-yl)ethanol). CB1954 (5-[aziridin-1-yl]-2,4-dinitrobenzamide) was purchased from MedKoo Bioscience (Morrinsville, NC). The prodrugs PR-104A (2-((2-bromoethyl)-2-{[(2-hydroxyethyl) amino]carbonyl}-4,6-dinitroanilino) ethylmethanesulfonate) and its di-bromo analogue SN27686, and nitro-CBI-DEI (nitro-CBI-5-[(dimethylamino)ethoxy]indole) were synthesised in-house at the Auckland Cancer Society Research Centre (Auckland, New Zealand).

2.2. Bacterial strains, genes and plasmids

Candidate nitroreductase genes were PCR-amplified from genomic DNA stocks and cloned into the ampicillin resistant expression plasmid pUCX or the kanamycin resistant His_6-tagged expression plasmid pET28a(+) as previously described ([24,23]. Genes encoding the NfsA and NfsB enzymes were cloned from *E. coli* strain W3110 [24] and the YfkO enzyme from a New Zealand isolate of *Bacillus subtilis* [25]. For recombinant protein purification, the *nfsA* gene in pET28a (+) was expressed in *E. coli* BL21 (DE3) cells. For screening we employed the *E. coli* strains 7NT and SOS-R4 as previously described [4] as activator and recipient cells, respectively. Both strains are isogenic derivatives of the *E. coli* strain W3110, which has seven endogenous nitroreductase candidate genes (*nfsA, nfsB, azoR, nemA, mdaB, yieF* and *ycaK*) deleted to reduce background activation of nitroaromatic prodrugs together with deletion of the *tolC* gene to restrict active efflux of unreduced prodrug. The SOS-R4 strain additionally contains a spectinomycin resistant plasmid bearing a green-fluorescent-protein-mut3 (GFP) reporter gene controlled by the SOS inducible *sfiA* promoter. To enable co-incubation of the activator and recipient strains the empty plasmid pCDFDuet was transformed into the 7NT strains to confer spectinomycin resistance.

2.3. SOS and bacterial bystander assays in 384 well microtitre plates

Evaluation of cell-to-cell transfer of activated prodrug metabolites in *E. coli* liquid cultures was initially performed in 384 well microtitre plates. Overnight cultures of a nitroreductase-expressing 7NT activator strain, a nitroreductase null 7NT control strain, and the SOS-R4 recipient strain were inoculated in 3 mL aliquots of LBASG media (lysogeny broth supplemented with 100 $\mu g.mL^{-1}$ ampicillin, 50 $\mu g.mL^{-1}$ spectinomycin and 0.2% glucose (w/v)) in sterile 15 mL centrifuge tubes and incubated overnight for 16 h at 30 °C with shaking at 200 rpm. The following morning, 0.5 mL of the overnight culture was used to inoculate a day culture of 10 mL of LBASGI (LBASG supplemented with 50 μM IPTG), which was then incubated at 30 °C, 200 rpm for 3 h. Prior to prodrug challenge all cultures were diluted using fresh LBASGI media to an OD_{600} of 0.8. In 384 well plates, pairs of wells were filled with either 30 μL control media (LBASGI only) or 30 μL challenge media (LBASGI supplemented with twice the desired final challenge concentration of the prodrug). To establish an activator to recipient ratio of 50:50, 15 μL of either the nitroreductase-expressing 7NT activator or the nitroreductase null 7NT control day cultures were added to each pair of wells, followed by addition of 15 μL of culture of the SOS-R4 recipient strain (alternatively, to establish an activator to recipient ratio of 10:90, 100 μL of activator culture and 900 μL of SOS-R4 recipient culture were mixed and then 30 μL was dispensed into the assigned microtitre wells). Individual controls of each test strain were also grown in both control and challenge media to enable background levels of growth inhibition and GFP expression to be ascertained. All cultures were then incubated at 30 °C, 200 rpm for 3.5 h, at which point OD_{600} and GFP fluorescence (excitation 488 nm/emission 510 nm) were measured on an Enspire™ 2300 Multilabel Reader (Perkin Elmer, Waltham, MA). To calculate the fold increase in fluorescence resulting from cell-to-cell transfer of activated prodrug metabolites, the average fluorescence of each test condition (i.e., using the nitroreductase-expressing 7NT activator strain) was divided by the average fluorescence of the corresponding control condition (i.e., using the nitroreductase null 7NT control strain). Six biological replicates were performed for each condition; each consisting of a minimum of four technical replicates (biological replicates were derived from independent overnight cultures, whereas technical replicates were individual microtitre cultures derived from a single overnight culture for each condition.

2.4. Bacterial bystander assays in flow cytometry

Flow cytometry was used to quantify the levels of GFP expression in individual cells immediately following evaluation of cell-to-cell transfer of activated prodrug metabolites for the entire population by the microtitre plate method. After the OD_{600} and GFP fluorescence were recorded for the 384 well plates, each set of technical replicates for each challenge condition was pooled. In individual 14 mL round-bottom

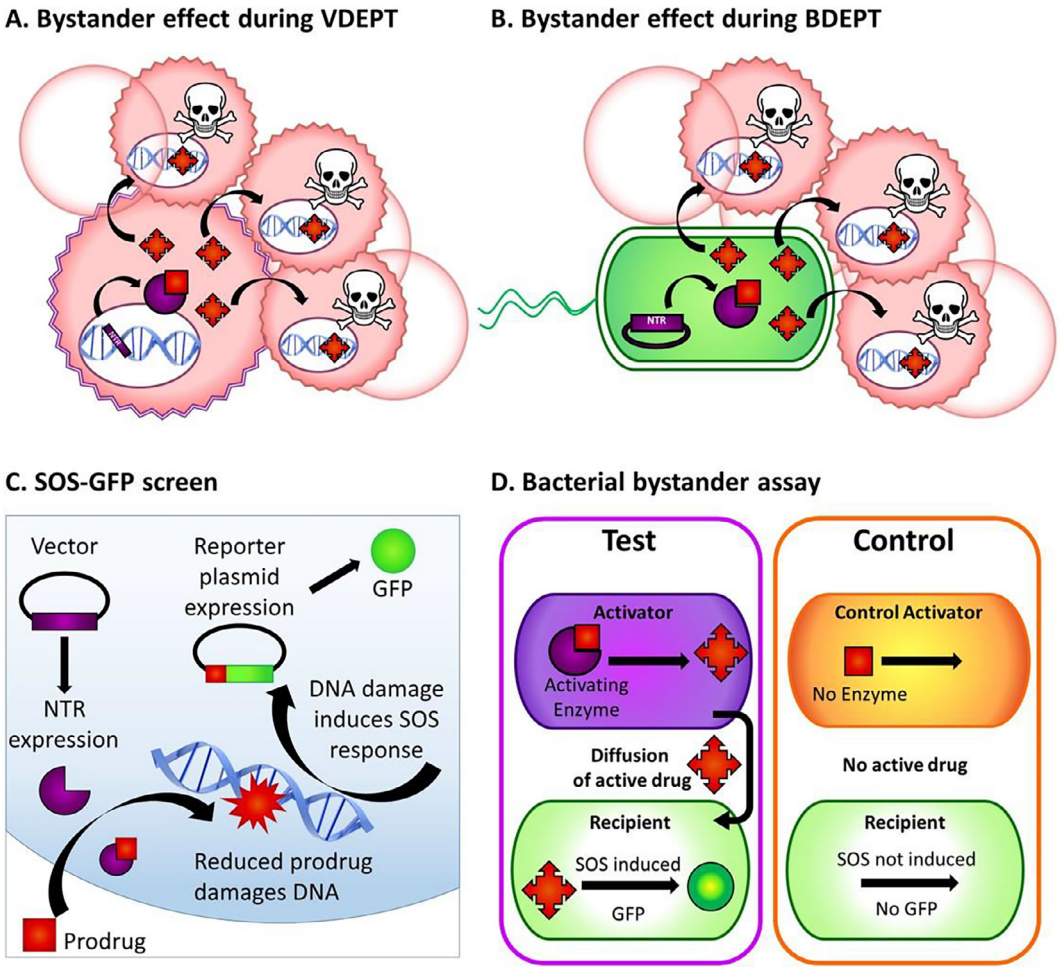

Fig. 1. Cell-to-cell transfer of activated prodrug metabolites in vivo and in vitro. A. Representation of the bystander effect in vivo during virus-directed enzyme-prodrug therapy (VDEPT). Gene (purple rectangle) delivery mediated by a tumour tropic viral vector leads to tumour-specific expression of the encoded nitroreductase enzyme (purple pacman), able to convert a nitroaromatic prodrug (red square) into a genotoxic form (red star). In this scenario the bystander effect involves transfer of the genotoxin from a transduced cancer cell into neighbouring untransduced cancer cells. **B. Representation of the bystander effect in vivo during bacteria-directed enzyme-prodrug therapy (BDEPT).** Gene delivery mediated by a tumour tropic bacterial vector leads to expression of the encoded nitroreductase enzyme within a bacterial cell residing in infected tumour tissue. The nitroreductase is able to convert a nitroaromatic prodrug (red square) into a highly genotoxic form (red star) inside the bacterial vector. In this scenario the bystander effect involves transfer of the genotoxin from the bacterial vector into surrounding cancer cells. **C. Basis of the SOS-GFP screen to detect DNA damage within E. coli reporter cells.** Nitroreductase (NTR) mediated activation of a nitroaromatic prodrug to a genotoxic form results in DNA damage (red explosion) and activation of the *E. coli* SOS response, detectable in reporter cells via induction of GFP (green circle) from a plasmid-based reporter. Prodrug activation can occur either internal (as depicted) or external to the reporter cell; in the latter scenario, the activated prodrug metabolites must be transferred into the reporter cell before induction of the SOS response will occur. **D. Schematic of the "bacterial bystander assay" to quantify bacterial cell-to-cell transfer of genotoxic metabolites.** In the test condition the nitroreductase-expressing 7NT activator cells (purple cell) convert the prodrug into a genotoxic product. The bacterial bystander assay monitors the efficiency of transfer of the genotoxin from the activator cells into co-cultured SOS-R4 recipients (green cell). The recipients quantify receipt of the genotoxin via GFP expression induced by DNA damage. The background level of toxicity caused by unconverted prodrug, or prodrug activated by other endogenous enzymes present in the activator or recipient cells, is measured using a nitroreductase-null 7NT control activator strain (orange cell) co-cultured with SOS-R4 recipients. The fold difference in GFP signal between the test and control conditions is a measure of the extent of bacterial cell-to-cell transfer of nitroreductase-activated prodrug metabolites.

polypropylene tubes, 25 µL of each challenge or control condition was diluted in 1 mL of PBS and mixed by vortexing for five seconds. Each sample was analysed on a Becton Dickinson FACSCanto II (BD Biosciences San Jose, CA), under the parameters: FSC 570, SSC 450 and GFP 555 within 2.5 h of removal from the incubator. The first sample analysed was always the unchallenged 7NT strain bearing an empty pUCX plasmid, to establish the level of background fluorescence for activator cells and allow a gate to be set immediately above this boundary. Subsequently, for each sample 30,000 fluorescent events were collected using a low flow rate of approximately 12 µL of sample per minute (BD LSR II User's Guide). A minimum of three experimental replicates were collected for each challenge condition and at least three independent biological repeats were performed for each final data set.

All data was processed using the Flowing Software version 2.5.1 by Perttu Terho (Turku Centre for Biotechnology, Turku, Finland) and Flowjo (© FlowJo, LLC, 2013–2018; BD Biosciences San Jose, CA). To calculate the fold increase in mean population fluorescence resulting from cell-to-cell transfer of activated prodrug metabolites, the average fluorescence of each test condition was divided by the average fluorescence of the corresponding control condition. In this flow cytometry based assay, biological replicates were derived from independent overnight cultures. Technical replicates were individual microtitre cultures derived from a single overnight culture that were then pooled and dispensed into PBS for flow cytometry assessment.

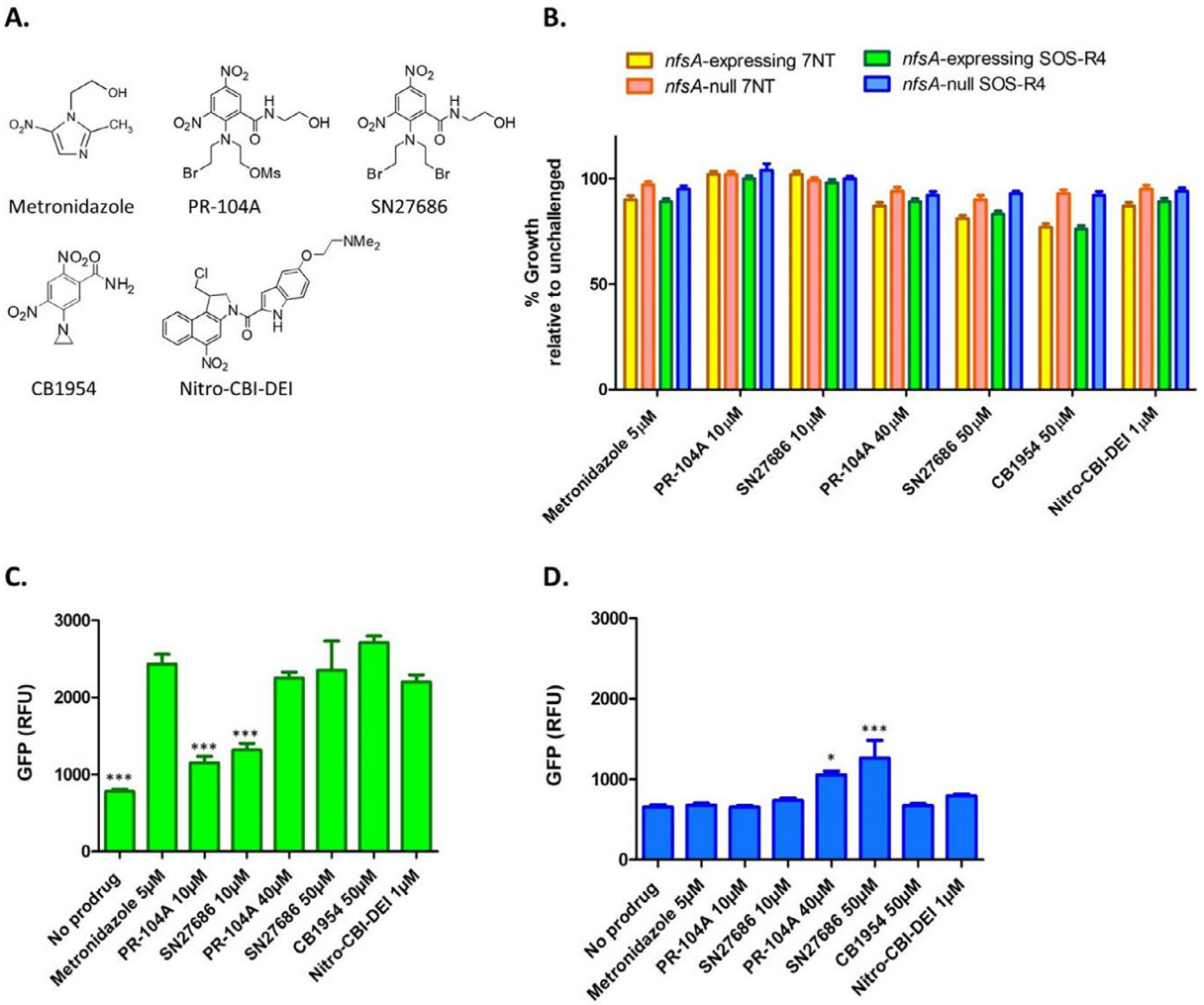

Fig. 2. Identification of nitroaromatic prodrugs and optimal concentrations for use in this study. A. Chemical structures of prodrugs studied in this work. B. Identification of prodrug concentrations resulting in < 20% growth inhibition of nitroreductase-expressing activator cells. Empirical testing identified promising prodrug concentrations of 5 μM metronidazole, 50 μM CB1954, 1 μM nitro-CBI-DEI, and either 10 μM or 40 μM PR-104A, and 10 μM or 50 μM SN27686. The effect of these prodrug concentrations on growth inhibition was tested for different strains used in this study: nfsA-expressing 7NT activators (yellow bars), nitroreductase null 7NT control (pink bars), nitroreductase null SOS-R4 recipients (blue bars), and an additional positive control of nfsA-expressing SOS-R4 (green bars). Data were derived from six biological replicates, each comprising a minimum of four technical replicate cultures grown in a 384 well microtiter plate. Error bars represent standard deviation of the average growth (OD600 represented as a percentage relative to unchallenged control cultures) across the six biological replicates. **C. Relative GFP fluorescence of nfsA-expressing SOS-R4 exposed to different prodrugs.** Levels of GFP fluorescence were measured following 3.5 h incubation of nfsA-expressing SOS-R4 challenged with each prodrug at 30 °C, 200 rpm. Data were derived from six biological replicates, each comprising a minimum of four technical replicate cultures grown in a 384 well microtiter plate. Error bars represent standard deviation of the average GFP (RFU) across the six biological replicates. *** indicates $p < 0.001$ (one-way repeated measures ANOVA with Tukey's post-hoc test) GFP signal is significantly different from that measured for the nil-bystander prodrug metronidazole. **D. Relative GFP fluorescence of nitroreductase null SOS-R4 recipients exposed to different prodrugs.** To evaluate the basal levels of genotoxicity for each prodrug in the absence of NfsA, SOS-R4 cells containing an empty plasmid were exposed to each prodrug, with data collected and presented as for Panel C. Error bars represent standard deviation of the average GFP (RFU) across the six biological replicates. * indicates $p < 0.05$ and *** indicates $p < 0.001$ (one-way repeated measures ANOVA with Tukey's post-hoc test) GFP signal is significantly different from no prodrug control.

2.5. Prodrug pre-activation assay

Recombinant NfsA was expressed from plasmid pET28a(+) as an N-terminal His_6 tagged enzyme and purified by nickel-affinity chromatography (Novagen, Merck, Darmstadt, Germany) with flavin reconstitution and buffer exchange as previously described [24]. Protein concentrations were calculated using a Nanodrop spectrophotometer and enzyme purity was confirmed by SDS-PAGE.

Subsequently the purified NfsA protein was used to pre-activate 200 μM PR-104A, 150 μM SN27686 or 125 μM of nitro-CBI-DEI. Reactions were performed in 60 μL in UVettes™ (Eppendorf, Hamburg, Germany), containing 10 mM Tris–Cl (pH 7.0), 4% DMSO, 3 mM NAD(P)H. Reactions were initiated by addition of 6 μL of 1 μg/μL NfsA enzyme to 54 μL of the appropriate substrate mixture, for a final concentration of 0.1 μg/μL of enzyme. The reaction was monitored in a 1 cm path length, using a Helios γUV–Vis spectrophotometer (Thermo Scientific, Middletown, VA) at 5 min intervals for 15–20 min until the reaction had gone to completion, i.e. no further change in absorbance was detected. Activation of the prodrug nitro-CBI-DEI was monitored by oxidation of the electron donating co-substrate NADPH at a wavelength of 340 nm as measured by a decrease in absorbance. For the mustard prodrugs PR-104A and SN27686 the formation of the reduced metabolite, from the parental substrate, can be detected by monitoring the decrease in absorbance at a wave length of 400 nM. At this wavelength there is no interference by reduced or oxidised NAD(P)H co-substrate.

The pre-activated prodrug metabolites were used to challenge cultures of the null-nitroreductase recipients. Overnight cultures of the

SOS-R4 recipient strain were inoculated in 3 mL aliquots of LBASG media in sterile 15 mL centrifuge tubes and incubated for 16 h at 30 °C with shaking at 200 rpm. The following morning, 0.5 mL of the overnight culture was used to inoculate a day culture of 10 mL of LBASGI which was then incubated at 30 °C, 200 rpm for 3 h. Prior to challenge with the pre-activated prodrug metabolites the SOS-R4 culture was diluted using fresh LBASGI media to an OD_{600} of 0.8. In 384 well plates eight technical replicate were created for each challenge condition. LBASGI media was used to dilute the pre-activated prodrug metabolites to the following concentrations: 80 μM for PR-104A, 100 μM for SN27686 and 2 μM for nitro-CBI-DEI in a volume of 30 μL. The challenge culture was inoculated by addition of 30 μL of the diluted SOS-R4 recipient strains to each of the wells; this diluted the pre-activated prodrug metabolites to the same final concentrations as used in the bystander effect assays. Control conditions for each condition were created by using a volume of 10 mM Tris–Cl (pH 7.0) buffer equivalent to that of the volume of the pre-activated prodrug metabolites. Prior to incubation the OD_{600} was measured on an Enspire™ 2300 Multilabel Reader (Perkin Elmer, Waltham, MA). All cultures were then incubated at 30 °C, 200 rpm for 3.5 h at which point the OD_{600} and GFP fluorescence was also recorded. To calculate the fold increase in fluorescence, resulting from transfer of activated prodrug metabolites from the media into the SOS-R4 cells, the average fluorescence of each challenge condition was divided by the average fluorescence of the corresponding control condition. Growth inhibition was also measured at 600 nm to ensure the acceptable limit of 20% growth inhibition of challenged cultures compared to unchallenged controls was not exceeded.

3. Results

3.1. Assay design

We previously reported the development of SOS-R4, a SOS (DNA damage responsive) GFP reporter strain of *E. coli*, and its utility for directed evolution to improve the bioreductive activation of nitroaromatic prodrugs by a target nitroreductase enzyme [4,5] (Fig. 1C). Here, we considered that SOS-R4 might also be able to report on the ability of genotoxic prodrug metabolites to exit a nitroreductase-expressing non-reporter strain of *E. coli* in liquid co-culture. By comparing the levels of GFP expression between SOS-R4 cells co-cultured with either a nitroreductase-expressing or a nitroreductase null 7NT strain (Fig. 1D), we reasoned that we could subtract any background levels of GFP induced by direct prodrug exposure.

We selected *E. coli* NfsA as the prodrug-converting enzyme, as previous studies have shown that this enzyme is an excellent generalist nitroreductase that has high-level activity across a range of nitroaromatic substrates [33,27]. Prodrugs were selected for this investigation to span a range of chemical structures (Fig. 2A) and on the basis of their bystander effects having previously been evaluated in mixed multilayer cell culture models. In order of ascending bystander effect in these models these were: metronidazole, negligible bystander effect [2,16]; CB1954, low bystander effect [30,26,31]; PR-104A and its more lipophilic di-bromo mustard analogue SN27686, medium to high bystander effects [26,10,21]; and nitro-CBI DEI, maximal bystander effect [32,13]. (Note: as the different studies that we refer to employed substantially different proportions of activator cells in their mixed multilayer cell culture models, it is not possible to directly compare the calculated bystander effect efficiencies of the different prodrug metabolites, and hence we have employed qualitative terms to describe their relative bystander efficiencies.)

We next sought to identify test concentrations for each prodrug that would enable meaningful comparisons to be made between the different molecules. It is known that different nitroaromatic prodrug metabolites can exhibit markedly different dose potencies [29], and we have previously found that a greater than 20% decrease in culture turbidity in response to prodrug challenge, relative to an unchallenged control, can cause a reduction in output from SOS reporter gene assays [24]. We therefore empirically selected concentrations of each prodrug that could elicit comparable levels of GFP expression in an SOS-R4 reporter strain expressing *nfsA*, without causing more than 20% growth inhibition of that strain. Pilot studies resulted in selection of the following test prodrug concentrations: 5 μM metronidazole, 50 μM CB1954, 40 μM PR-104A, 50 μM SN27686, and 1 μM nitro-CBI-DEI. At these selected prodrug concentrations growth inhibition was in the allowable range for all bacterial strains used. We observed that at these concentrations the reduction in culture turbidity relative to an unchallenged control was similar for both 7NT and SOS-R4 strains expressing *nfsA* (and in all cases < 20%), and that nitroreductase null 7NT and SOS-R4 strains exhibited little to no growth inhibition (Fig. 2B). The relative levels of GFP expression in the *nfsA*-expressing SOS-R4 strain were similar for all prodrugs at these concentrations (Fig. 2C), however we additionally noted that the dinitrobenzamide mustard prodrugs PR-104A and SN27686 caused a statistically significant induction of GFP in a nitroreductase null strain of SOS-R4 at the selected test concentrations of 40 μM and 50 μM respectively compared to the no prodrug control (Fig. 2D). This indicates that at these concentrations the two prodrugs were causing a significant SOS DNA damage response despite the absence of an activating nitroreductase. To allow for the possibility that this low-level background might influence assay results, we therefore also tested PR-104A and SN27686 at 10 μM apiece throughout this work. After retesting the *nfsA*-expressing SOS-R4 strain at these lower prodrug concentrations, we found that the PR-104A and SN27686 at 10 μM generated significantly lower GFP signals than the metronidazole control (Fig. 2B) but did not induce a statistically significant SOS DNA damage response in the absence of a nitroreductase (Fig. 2D).

3.2. Bacterial bystander microtitre plate assay

We first evaluated the ability of our activated prodrug metabolites to be transferred from activator to recipient cells in a microtitre plate assay format. Nitroreductase null SOS-R4 recipient cells were co-cultured at a 1:1 ratio with either *nfsA*-expressing 7NT activator cells (test condition) or nitroreductase-null 7NT cells (control condition). Following exposure to each prodrug, cell-to-cell transfer of genotoxic metabolites was quantified by monitoring the mean fold-increase in fluorescence for the test condition relative to the control (Fig. 3). Consistent with the bystander effects previously observed in human tumour mixed multilayer cell culture models, reduction of metronidazole by *nfsA*-expressing 7NT activator cells did not induce significant levels of GFP in SOS-R4 recipients, whereas nitro-CBI-DEI caused a significant ($p < 0.001$) increase in fluorescence. Surprisingly, CB1954 also caused a significant ($p < 0.001$) increase in fluorescence, despite having exhibited only a weak bystander effect in human cell models [30,32,26]. In contrast, the dinitrobenzamide mustard prodrugs, which exhibited substantially higher bystander effects than CB1954 in human cell models, induced only slightly higher levels of GFP in the SOS-R4 recipients than metronidazole. The bystander effects of the mustard prodrugs were not significantly different from metronidazole irrespective of whether the 10 μM or higher challenge concentration was applied. Relative to PR-104A (logP = 1.0) the more lipophilic (di-bromo-mustard) analogue SN27686 (logP = 2.3) appeared to induce higher levels of GFP in SOS-R4 cells, however this difference was not significant.

To confirm that the lack of GFP induction by the activated metabolites of the two dinitrobenzamide mustard prodrugs was indeed due to inability to exit the 7NT activator cells, we incubated each prodrug with purified NfsA enzyme and NADPH *in vitro*, then added the mixture 1:1 to a culture of SOS-R4 cells. This resulted in a significant ($p < 0.001$) SOS DNA damage response in the nitroreductase null SOS-R4 recipients incubated with pre-activated mustard prodrugs as well as pre-activated nitro-CBI-DEI compared to the no prodrug controls

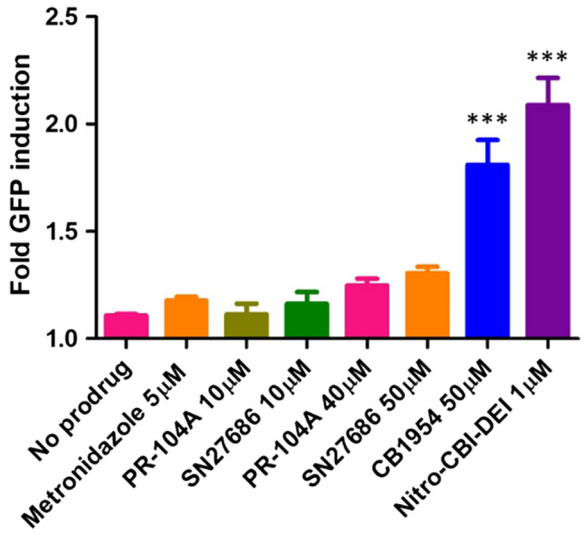

Fig. 3. Microplate assay of SOS response induced by transfer of activated prodrug metabolites from nfsA-expressing 7NT activator cells to nitroreductase null SOS-R4 reporter cells. 50:50 mixed cultures of nfsA-expressing 7NT activator cells and SOS-R4 recipients were incubated with either 5 μM metronidazole, 50 μM CB1954, 1 μM nitro-CBI-DEI, 10 μM or 40 μM PR-104A, or 10 μM or 50 μM SN27686 for 3.5 h, at which point GFP fluorescence (excitation 490 nm/emission 530 nm) was measured. The bacterial bystander effect was measured by the fold increase in GFP expression of the test condition over the control condition. Six biological replicates were performed each comprising eight technical replicates for test and control conditions. Error bars represent standard deviation of the average fold increase in GFP induction across the six biological replicates. *** indicates $p < 0.001$ (one-way repeated measures ANOVA with Tukey's post-hoc test) relative to no prodrug control.

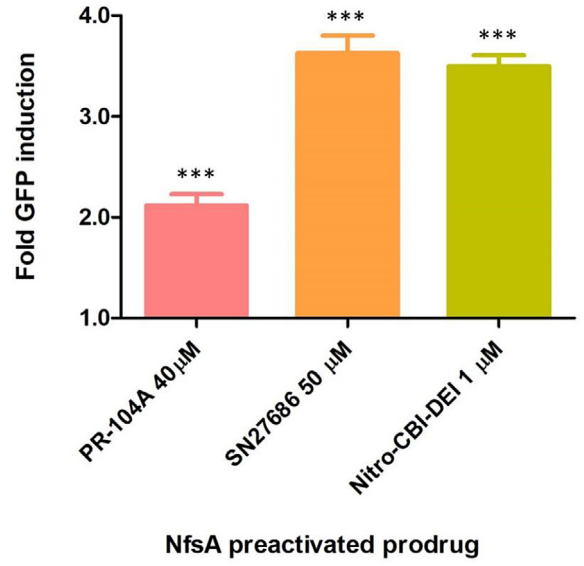

Fig. 4. Microplate assay of SOS response induced by transfer of pre-activated prodrug metabolites to nitroreductase null SOS-R4 reporter cells. 30 μL cultures of SOS-R4 recipients were incubated with either 40 μM PR-104A, 50 μM SN27686 or 1 μM nitro-CBI-DEI that had been pre-activated by incubation in vitro with purified NfsA enzyme and excess NADPH, after which GFP fluorescence was measured. The transfer of the pre-activated prodrug metabolite from the surrounding media into the SOS-R4 recipients was detected by the fold increase in GFP expression relative to an unchallenged control condition. A minimum of three biological replicates were performed (each comprising at least four technical replicates), and error bars represent standard deviation across the three biological replicates. *** indicates $p < 0.001$ (one-way repeated measures ANOVA with Tukey's *post-hoc* test) relative to the unchallenged control.

(Fig. 4). This observation ruled out the possibility of compound-specific neutralisation in the LB growth medium or inability of the dinitrobenzamide mustards to penetrate the SOS-R4 recipient cells.

3.3. Bacterial bystander flow cytometry assay

Whereas plate reader assays measure the mean fluorescence of an entire population of cells, flow cytometry approaches can provide additional information on the variance between individual cells in that population. Here, *nfsA*-expressing 7NT activator cells or nitroreductase null 7NT cells were mixed 1:1 with SOS-R4 recipient cells, exposed to prodrug, and analysed by flow cytometry. For each prodrug, fluorescence histograms were derived from gated reads of 30,000 recipient cells apiece for the test and control conditions. When paired histograms were overlaid, no clear differences could be observed between the test and control for either the no prodrug control or for 5 μM metronidazole (Fig. 5A). From these panels it was also evident that although there was substantial variation in the fluorescence of individual SOS-R4 recipient cells, at a population level the distribution of fluorescence was highly consistent. For the remaining prodrugs, the histogram overlay plots were also congruent with the plate reader data: 50 μM CB1954 and 1 μM nitro-CBI-DEI both caused strong shifts in SOS-R4 fluorescence, indicating high levels of cell-to-cell transfer of activated prodrug metabolites, whereas PR-104A and SN27686 caused minimal shifts in SOS-R4 fluorescence at either challenge concentration (Fig. 5A). The fluorescence histograms confirmed that 40 μM PR-104A and 50 μM SN27686 were causing activation of GFP expression in SOS-R4 cells even in the absence of the *nfsA*-expressing activator strain (as previously observed in microplate assays; Fig. 2D). However, this high GFP background does not appear to have been the reason for the failure to detect cell-to-cell transfer of the activated metabolites of these prodrugs, given the lack of background yet minimal fluorescence shift when each dinitrobenzamide mustard was tested at 10 μM (Fig. 5A). The mean population fluorescence for each condition across all repeats is summarised in Fig. 5B. As in the microplate assay, CB1954 and nitro-CBI-DEI were the only prodrugs that induced statistically significant ($p < 0.001$) increases in GFP induction compared to the null bystander effect metronidazole condition.

3.4. The bystander effect of CB1954 is dependent on the reduction product (s)

The ability of the reduced metabolites of CB1954 to exit our *nfsA*-expressing 7NT activator strain and induce GFP expression in our SOS-R4 recipient strain was substantially stronger than we had expected based on previous studies of bystander effect in human carcinoma 3D mixed multicellular models [30,26,31]. One possible explanation for this was our choice of NfsA as the prodrug-converting nitroreductase, in contrast to the NfsB enzyme that was used in the 3D cell culture studies. Whereas NfsB can reduce either the 2-NO_2 or the 4-NO_2 groups of CB1954, in an approximately equimolar ratio [1,14], NfsA reduces CB1954 exclusively at the 2-NO_2 position [28,24]. It has been shown in human cervical cancer (SiHa) cells expressing *nfsB* that the products of reduction at the 4-NO_2 position exhibit a substantially lower bystander effect than the 2-NO_2 reduction products [14]. Consistent with this, untransfected ovarian carcinoma (SKOV3) cells were found to be more sensitive to CB1954 when co-cultured with *nfsA*-expressing cells than when they were co-cultured with *nfsB*-expressing cells [28].

We therefore sought to compare the effects of using *nfsA versus nfsB* as the prodrug-converting nitroreductase gene in our 7NT activator cells. To enable a more precise assessment of the ability of the 2-NO_2 *versus* 4-NO_2 reduction products of CB1954 to activate the SOS response in our SOS-R4 recipient cells, we also generated a third activator strain, 7NT cells expressing the nitroreductase gene *yfkO* from *Bacillus subtilis*. We have previously shown that YfkO is an efficient nitroreductase that reduces CB1954 exclusively at the 4-NO_2 position [25] and that the

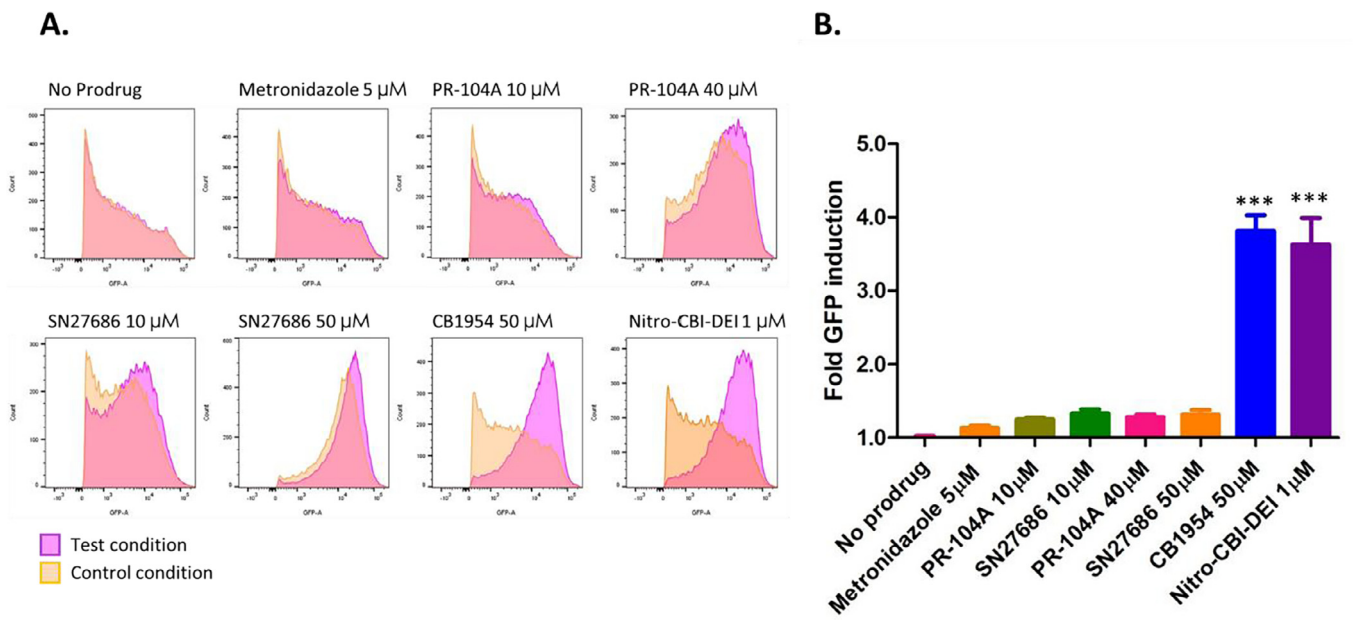

Fig. 5. Flow cytometry analysis of DNA damage caused by transfer of activated prodrug metabolites from nfsA-expressing 7NT activator cells to nitroreductase null SOS-R4 reporter cells. A. Overlay histograms of test and control conditions. 50:50 mixed cultures of SOS-R4 recipients and either nitroreductase null 7NT control cells or nfsA-expressing 7NT activator cells were incubated with either 5 μM metronidazole, 50 μM CB1954, 1 μM nitro-CBI-DEI, 10 μM or 40 μM PR-104A, or 10 μM or 50 μM SN27686 for 3.5 h in eight technical replicates apiece. The eight replicates were then pooled and 25 μL of each pooled sample measured for GFP fluorescence using flow cytometry. The collection gate was set at the GFP region above the background fluorescence of the nitroreductase null 7NT control strain under no prodrug conditions. Overlay histograms are representative technical replicates that indicate the population fluorescence of 30,000 events for the mixture containing the nitroreductase null 7NT strain (Control condition; orange) or the *nfsA*-expressing 7NT activator cells (Test condition; pink). **B. Mean increase in GFP signal of test condition over control condition.** Six biological replicates were performed for each condition indicated in Panel A. For each, the GFP geomean of at least three technical replicates was averaged and the bacterial bystander effect was quantified as the average fold increase in GFP fluorescence for the test condition over the control condition. Error bars represent standard deviation of the average fold increase in GFP induction across the six biological replicates, and *** indicates $p < 0.001$ (one-way repeated measures ANOVA with Tukey's *post-hoc* test). (For interpretation of the references to colour in this figure legend, the reader is referred to the web version of this article.)

nfsA, *nfsB*, and *yfkO* genes all express protein at similar levels from plasmid pUCX in *E. coli* [23].

7NT activator cells expressing *nfsA, nfsB* or *yfkO* or nitroreductase-null 7NT cells were mixed 1:1 with SOS-R4 recipient cells, challenged with 50 μM CB1954, and analysed by flow cytometry. There was little to no difference in GFP profiles between the overlay histograms for the *nfsA* and *nfsB* expressing activator strains (Fig. 6A, B). Although NfsA and NfsB induced levels of GFP that were significantly greater ($p < 0.01$ and $p < 0.05$ respectively) than YfkO, the two *E. coli* derived nitroreductases were not significantly different from each other (Fig. 6B). Thus, the strong induction of GFP expression in our CB1954 assays could not be attributed to our selection of NfsA as the prodrug converting nitroreductase. In contrast, the *yfkO*-expressing activator strain caused only a small increase in SOS-R4 population fluorescence relative to the nitroreductase-null control (Fig. 6A, B), confirming our expectations that the 4-NO_2 reduced metabolites of CB1954 exhibit poor cell-to-cell transfer in bacteria as well as cultured human cells (Fig. 6B).

To further investigate whether the lack of substantial difference between the *nfsA* and *nfsB* expressing activator strains may have been due to saturation of fluorescence in the SOS-R4 recipients, we reduced the ratio of activator to recipient cells in our assay co-cultures from 1:1 to 1:9. As expected the overall levels of fluorescence for each co-culture greatly decreased, reflecting the reduced number of nitroreductase expressing cells in the assay (Fig. 6C, D). Under these conditions there was a significant difference between the NfsA and YfkO conditions ($p < 0.01$) but not between NfsB and YfkO.

4. Discussion

The bystander effects of diverse nitroaromatic prodrug metabolites have previously been evaluated in mixed multilayer carcinoma cell models, comparing the survival of untransduced target cells in the presence or absence of co-incubated nitroreductase-expressing activator cells. This multilayer model simulates tissue-like cell densities and can explicitly test the ability of activated metabolites to diffuse through tumour tissue [30]. These qualities make the model highly appropriate for modelling VDEPT scenarios, where infected human cells yield prodrug products from intracellular catalytic processes. However, the physiology of bacterial cells differs substantially from human cells, and we considered that the same prodrug metabolites might vary in their relative abilities to exit a bacterial activator cell. To establish a more relevant model for cell-to-cell transfer of activated prodrug metabolites in BDEPT we adapted a GFP-SOS reporter strain of *E. coli* to monitor the transfer of genotoxic prodrug metabolites from a co-cultured activator strain, rather than activation of prodrugs by an endogenous nitroreductase as previously described [4,5].

We recognise that our experimental model employs a large liquid to cell volume ratio, which may not reproduce the potentially close association of bacterial vectors to cancer cells in clinical BDEPT. However, studying the effects of prodrug activation by bacterial activator cells in co-culture with target carcinoma cells would be confounded by the naturally oncolytic nature of bacteria, which would cause death of the target cells by numerous prodrug-independent mechanisms [11,23]. Our model is robust and easily implemented, and importantly it does inform on the relative abilities of prodrug metabolites to exit bacterial activator cells. Moreover, as we have shown, addition of prodrug metabolites activated by a purified nitroreductase in vitro can be used to control for the possibility that these metabolites might be unstable and neutralised by components of the culture medium, or fail to penetrate the SOS-R4 reporter cells.

As our model employs *E. coli* activator cells we consider that it is

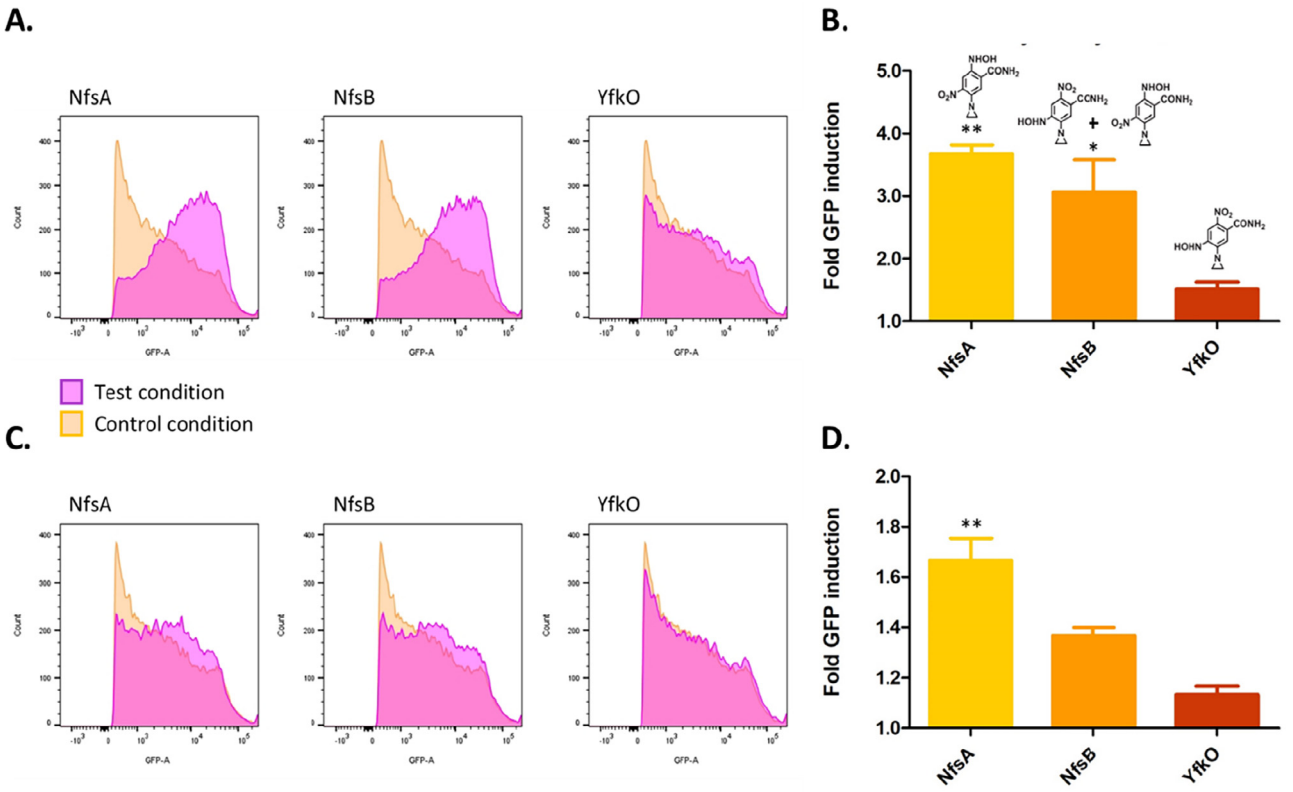

Fig. 6. Flow cytometry analysis of DNA damage caused by transfer of activated prodrug metabolites from *nfsA*, *nfsB* or *yfkO* -expressing 7NT activator cells to nitroreductase null SOS-R4 reporter cells. A. Overlay histograms of test and control conditions for a 50% activator cell population. 50:50 mixed cultures of SOS-R4 recipients and either nitroreductase null 7NT control cells or *nfsA*, *nfsB* or *yfkO* -expressing 7NT activator cells were incubated with either no prodrug or 50 μM CB1954 for 3.5 h in eight technical replicates apiece. The eight replicates were then pooled and 25 μL of each pooled sample measured for GFP fluorescence using flow cytometry. Overlay histograms indicate the population fluorescence of 30,000 events for the mixture containing the nitroreductase null 7NT strain (Control condition; orange) or the *nfsA*, *nfsB* or *yfkO* -expressing 7NT activator cells (Test condition; pink). **B. Mean increase in GFP signal of test condition over control condition for a 50% activator cell population.** Three biological replicates were performed each comprising a minimum of three technical replicates for each test and control condition indicated in Panel A. For each, the GFP geomean of the three technical replicates was averaged and the bacterial bystander effect was quantified as the average fold increase in GFP fluorescence for the test condition over the control condition. A fold induction of GFP approaching one indicates a poor bacterial bystander effect. Error bars represent standard deviation of the average fold increase in GFP induction across the three biological replicates, and ** indicates $p < 0.01$ (one-way ANOVA Tukey test) GFP signal is significantly different from YfkO. **C. Overlay histograms of test and control conditions for a 10% activator cell population.** As per Panel A, but with 90:10 mixed cultures of SOS-R4 recipients and either nitroreductase null 7NT control cells or *nfsA*, *nfsB* or *yfkO*-expressing 7NT activator cells. **D. Mean increase in GFP signal of test condition over control condition for a 10% activator cell population.** As per Panel B, but with 90:10 mixed cultures of SOS-R4 recipients and either nitroreductase null 7NT control cells or *nfsA*, *nfsB* or *yfkO*-expressing 7NT activator cells. ** indicates $p < 0.01$ (one-way repeated measures ANOVA with Tukey's *post-hoc* test) GFP signal is significantly different from YfkO. (For interpretation of the references to colour in this figure legend, the reader is referred to the web version of this article.)

most relevant to *E. coli* and *Salmonella* vectors for BDEPT, rather than obligate anaerobes such as *Clostridium* or *Bifidobacteria*, owing to the inherent differences between Gram negative and Gram positive cell walls. For example, it is possible that the Gram positive cell wall might pose less of a barrier to the activated metabolites of dinitrobenzamide mustard prodrugs such as PR-104A and its analogues. Maintenance of an active TolC outer-membrane efflux channel might improve the ability of Gram negative bacterial vectors to redistribute these activated metabolites, but because PR-104A is itself rapidly effluxed by TolC [23], this would necessitate substantially higher concentrations of prodrug to render BDEPT effective, likely exceeding the dose that can be safely administered to patients (only 270 mg/m^2 for PR-104, the pre-prodrug form of PR-104A) [18]. We note it is also possible that the surprisingly poor cell-to-cell transfer we observed for the activated metabolites of PR-104A and SN27686 stems from a more generic feature of prokaryotic genome architecture. Unlike in a human activator cell, bacterial DNA is not coiled around histones or compartmentalised in a nucleus, and thus is more exposed to a cytoplasm-activated genotoxin. This may cause it to act as a sink for the activated mustards, which exhibit particularly high levels of alkylating reactivity [15], restricting cell-to-cell transfer relative to the less reactive metabolites of nitro-CBI-DEI and (2-nitro reduced) CB1954.

Whereas the relative absence of a bystander effect exhibited by 4-nitro reduced (i.e., YfkO-activated) CB1954 was consistent with previous studies in human carcinoma multicellular layers [14], we observed surprisingly high levels of cell-to-cell transfer for 2-nitro reduced CB1954, approaching those of reduced nitro-CBI-DEI. In contrast, NfsB-activated CB1954 exhibits only a weak bystander effect in human multicellular layers [30,26,20]). Our data therefore suggest that CB1954 may be a more effective prodrug for BDEPT applications (those employing Gram negative vectors, at least) than it has previously indicated in clinical VDEPT trials [3,22]. Based on this, we consider that CB1954 in combination with NfsA (or variants engineered for superior efficacy at the concentrations of this prodrug that are achievable in patients) may be worthy of further investigation in engineered *Salmonella* or *E. coli* BDEPT systems, leveraging the previous clinical development of this prodrug. Above all else, our results highlight the importance of evaluating enzyme-prodrug combinations in models relevant to the intended GDEPT vector, as there can evidently be profound differences in efficacy in different settings. Taking into account

the fundamental physiological differences associated with different gene-delivery systems will facilitate the identification of optimal enzyme-prodrug combinations for each setting.

Acknowledgements

This work was supported in part by grants from the Royal Society of New Zealand Marsden Fund (15-VUW-037 to D.F.A. and 07-VUW-080 to D.F.A. and A.V.P. in collaboration with J.N.C. and J.B.S.). J.V.E.C.-H. was supported by a Victoria University of Wellington PhD Scholarship. The authors thank Dr Moana Tercel for her generous gift of nitro-CBI-DEI prodrug.

References

[1] G.M. Anlezark, R.G. Melton, R.F. Sherwood, B. Coles, F. Friedlos, R.J. Knox, The bioactivation of 5-(aziridin-1-yl)-2,4-dinitrobenzamide (CB1954)-I. Purification and properties of a nitroreductase enzyme from *Escherichia coli*-A potential enzyme for antibody-directed enzyme prodrug therapy (ADEPT), Biochem. Pharmacol. 44 (1992) 2289–2295.

[2] J.A. Bridgewater, R.J. Knox, J.D. Pitts, M.K. Collins, C.J. Springer, The bystander effect of nitroreductase/CB1954 enzyme/prodrug system is due to cell permeable metabolite, Hum. Gene Ther. 8 (1997) 709–717.

[3] G. Chung-Faye, D. Palmer, D. Anderson, J. Clark, M. Downes, J. Baddeley, S. Hussain, P.I. Murray, P. Searle, L. Seymour, P.A. Harris, D. Ferry, D.J. Kerr, Virus-directed enzyme prodrug therapy with nitroimidazole reductase: a phase I and pharmacokinetic study of its prodrug, CB1954, Clin. Cancer Res. 7 (2001) 2662–2668.

[4] J.N. Copp, E.M. Williams, M.H. Rich, A.V. Patterson, J.B. Smaill, D.F. Ackerley, Toward a high-throughput screening platform for directed evolution of enzymes that activate genotoxic prodrugs, Protein Eng. Des. Sel. 27 (2014) 399–403.

[5] J.N. Copp, A.M. Mowday, E.M. Williams, C.P. Guise, A. Ashoorzadeh, A.V. Sharrock, J.U. Flanagan, J.B. Smaill, A.V. Patterson, D.F. Ackerley, Engineering a multifunctional nitroreductase for improved activation of prodrugs and PET probes for cancer gene therapy, Cell Chem. Biol. 24 (2017) 391–403.

[6] G.U. Dachs, M.A. Hunt, S. Syddall, D.C. Singleton, A.V. Patterson, Bystander or no bystander for gene directed enzyme prodrug therapy, Molecules 14 (2009) 4517–4545.

[7] W.A. Denny, W.R. Wilson, Bioreducible mustards: a paradigm for hypoxia-selective prodrugs of diffusible cytotoxins (HPDCs), Cancer Metastasis Rev. 12 (1993) 135–151.

[8] S. Duarte, G. Carle, H. Faneca, M.C.P. de Lima, V. Pierrefite-Carle, Suicide gene therapy in cancer: where do we stand now? Cancer Lett. 324 (2012) 160–170.

[9] Y. Flores Bueso, P. Lehouritis, M. Tangney, In situ biomolecule production by bacteria; a synthetic biology approach to medicine, J. Control. Release 275 (2018) 217–228.

[10] A. Foehrenbacher, K. Patel, M.R. Abbattista, C.P. Guise, T.W. Secomb, W.R. Wilson, K.O. Hicks, The role of bystander effects in the antitumor activity of the hypoxia-activated prodrug PR-104, Front. Oncol. 3 (2013) 1–18.

[11] N.S. Forbes, Engineering the perfect (bacterial) cancer therapy, Nat. Rev. Cancer 10 (2010) 785–794.

[12] S.M. Freeman, C.N. Abboud, K.A. Whartenby, C.H. Packman, D.S. Koeplin, F.L. Moolten, G.N. Abraham, The “bystander effect”: tumor regression when a fraction of the tumor mass is genetically modified, Cancer Res. 53 (1993) 5274–5283.

[13] L.K. Green, S.P. Syddall, K.M. Carlin, G.D. Bell, C.P. Guise, A.M. Mowday, M.P. Hay, J.B. Smaill, A.V. Patterson, D.F. Ackerley, *Pseudomonas aeruginosa* NfsB and nitro-CBI-DEI – a promising enzyme/prodrug combination for gene directed enzyme prodrug therapy, Mol. Cancer 12 (2013) 58.

[14] N.A. Helsby, D.M. Ferry, A.V. Patterson, S.M. Pullen, W.R. Wilson, 2-Amino metabolites are key mediators of CB 1954 and SN 23862 bystander effects in nitroreductase GDEPT, Br. J. Cancer 90 (2004) 1084–1092.

[15] N.A. Helsby, S.J. Wheeler, F.B. Pruijn, B.D. Palmer, S. Yang, W.A. Denny, W.R. Wilson, Effect of nitroreduction on the alkylating reactivity and cytotoxicity of the 2,4-dinitrobenzamide-5-aziridine CB1954 and the corresponding nitrogen mustard SN23862: distinct mechanisms of bioreductive activation, Chem. Res. Toxicol. 16 (2003) 469–478.

[16] M.A. Hunt, D. Li, M.P. Hay, M.J. Currie, B.A. Robinson, A.V. Patterson, G.U. Dachs, Characterisation of enzyme prodrug gene therapy combinations in coated spheroids and vascular networks in vitro, J. Gene Med. 14 (2012) 62–74.

[17] P. Lehouritis, G. Hogan, M. Tangney, Designer bacteria as intratumoural enzyme biofactories, Adv. Drug Deliv. Rev. 118 (2017) 8–23.

[18] M.J. McKeage, Y. Gu, W.R. Wilson, A. Hill, K. Amies, T.J. Melink, M.B. Jameson, A phase I trial of PR-104, a pre-prodrug of the bioreductive prodrug PR-104A, given weekly to solid tumour patients, BMC Cancer 11 (2011) 432.

[19] M. Mesnil, H. Yamasaki, Bystander effect in herpes simplex virus-thymidine kinase/ganciclovir cancer gene therapy: role of gap-junctional intercellular communication, Cancer Res. 60 (2000) 3989–3999.

[20] A.M. Mowday, A. Ashoorzadeh, E.M. Williams, J.N. Copp, S. Silva, M.R. Bull, M.R. Abbattista, R.F. Anderson, J.U. Flanagan, C.P. Guise, D.F. Ackerley, J.B. Smaill, A.V. Patterson, Rational design of an AKR1C3-resistant analog of PR-104 for enzyme-prodrug therapy, Biochem. Pharmacol. 116 (2016) 176–187.

[21] A.M. Mowday, C.P. Guise, D.F. Ackerley, N.P. Minton, P. Lambin, L.J. Dubois, J. Theys, J.B. Smaill, A.V. Patterson, Advancing clostridia to clinical trial: past lessons and recent progress, Cancers. 8 (2016) 1–14.

[22] P. Patel, J.G. Young, V. Mautner, D. Ashdown, S. Bonney, R.G. Pineda, S.I. Collins, P.F. Searle, D. Hull, E. Peers, J. Chester, D.M. Wallace, A. Doherty, H. Leung, L.S. Young, N.D. James, A phase I/II clinical trial in localized prostate cancer of an adenovirus expressing nitroreductase with CB1954, Mol. Ther. 17 (2009) 1292–1299.

[23] G.A. Prosser, J.N. Copp, A.M. Mowday, C.P. Guise, S.P. Syddall, E.M. Williams, C.N. Horvat, P.M. Swe, A. Ashoorzadeh, W.A. Denner, J.B. Smaill, A.V. Patterson, D.F. Ackerley, Creation and screening of a multi-family bacterial oxidoreductase library to discover novel nitroreductases that efficiently activate the bioreductive prodrugs CB1954 and PR-104A, Biochem. Pharmacol. 85 (2013) 1091–1103.

[24] G.A. Prosser, J.N. Copp, S. Syddall, E.M. Williams, J.B. Smaill, W.R. Wilson, A.V. Patterson, D.F. Ackerley, Discovery and evaluation of *Escherichia coli* nitroreductases that activate the anti-cancer prodrug CB1954, Biochem. Pharmacol. 79 (2010) 678–687.

[25] G.A. Prosser, A.V. Patterson, D.F. Ackerley, *uvrB* gene deletion enhances SOS chromotest sensitivity for nitroreductases that preferentially generate the 4-hydroxylamine metabolite of the anti-cancer prodrug CB1954, J. Biotechnol. 150 (2010) 190–194.

[26] D.C. Singleton, D. Li, S.Y. Bai, S.P. Syddall, J.B. Smaill, Y. Shen, W.A. Denny, W.R. Wilson, A.V. Patterson, The nitroreductase prodrug SN 28343 enhances the potency of systemically administered armed oncolytic adenovirus ONYX-411NTR, Cancer Gene Ther. 14 (2007) 953–967.

[27] B. Valiauga, E.M. Williams, D.F. Ackerley, N. Čėnas, Reduction of quinones and nitroaromatic compounds by *Escherichia coli* nitroreductase A (NfsA): characterization of kinetics and substrate specificity, Arch. Biochem. Biophys. 614 (2017) 14–22.

[28] S.O. Vass, D. Jarrom, W.R. Wilson, E.I. Hyde, P.F. Searle, *E. coli* NfsA: an alternative nitroreductase for prodrug activation gene therapy in combination with CB1954, Br. J. Cancer 100 (2009) 1903–1911.

[29] E.M. Williams, R.F. Little, A.M. Mowday, M.H. Rich, J.V.E. Chan-Hyams, J.N. Copp, J.B. Smaill, A.V. Patterson, D.F. Ackerley, Nitroreductase gene-directed enzyme prodrug therapy: insights and advances toward clinical utility, Biochem. J 471 (2015) 131–153.

[30] W.R. Wilson, S.M. Pullen, A. Hogg, N.A. Helsby, K.O. Hicks, W.A. Denny, Quantitation of bystander effects in nitroreductase suicide gene therapy using three-dimensional cell cultures, Cancer Res. 62 (2002) 1425–1432.

[31] W.R. Wilson, K.O. Hicks, S.M. Pullen, D.M. Ferry, N.A. Helsby, A.V. Patterson, Bystander effects of bioreductive drugs: potential for exploiting pathological tumor hypoxia with dinitrobenzamide mustards, Radiat. Res. 167 (2007) 625–636.

[32] W.R. Wilson, S.M. Stribbling, F.B. Pruijn, S.P. Syddall, A.V. Patterson, H.D.S. Liyanage, E. Smith, K.J. Botting, M. Tercel, Nitro-chloromethylbenzindolines: hypoxia-activated prodrugs of potent adenine N3 DNA minor groove alkylators, Mol. Cancer Ther. 8 (2009) 2903–2913.

[33] S. Zenno, H. Koike, A.N. Kumar, R. Jayaraman, M. Tanokura, K. Saigo, Biochemical characterization of NfsA, the *Escherichia coli* major nitroreductase exhibiting a high amino acid sequence homology to Frp, a *Vibrio harveyi* flavin oxidoreductase, J. Bacteriol. 178 (1996) 4508–4514.